

# Damage detection in truss bridges using transmissibility and machine learning algorithm: Application to Nam O bridge

Duong Huong Nguyen<sup>1,2a</sup>, H. Tran-Ngoc<sup>1,3a</sup>, T. Bui-Tien<sup>3b</sup>,  
Guido De Roeck<sup>4b</sup> and Magd Abdel Wahab<sup>\*5,6</sup>

<sup>1</sup> Department of Electrical energy, metals, mechanical constructions and systems,  
Faculty of Engineering and Architecture, Ghent University, Belgium

<sup>2</sup> Department of Bridge and Tunnel Engineering, Faculty of Bridge and Road, National University of Civil Engineering, Hanoi, Vietnam

<sup>3</sup> Department of Bridge and Tunnel Engineering, Faculty of Civil Engineering, University of Transport and Communications, Hanoi, Vietnam

<sup>4</sup> Department KU Leuven, Department of Civil Engineering, Structural Mechanics, B-3001 Leuven, Belgium

<sup>5</sup> Division of Computational Mechanics, Ton Duc Thang University, Ho Chi Minh City, Vietnam

<sup>6</sup> Faculty of Civil Engineering, Ton Duc Thang University, Ho Chi Minh City, Vietnam

(Received August 13, 2019, Revised January 3, 2020, Accepted March 30, 2020)

**Abstract.** This paper proposes the use of transmissibility functions combined with a machine learning algorithm, Artificial Neural Networks (ANNs), to assess damage in a truss bridge. A new approach method, which makes use of the input parameters calculated from the transmissibility function, is proposed. The network not only can predict the existence of damage, but also can classify the damage types and identify the location of the damage. Sensors are installed in the truss joints in order to measure the bridge vibration responses under train and ambient excitations. A finite element (FE) model is constructed for the bridge and updated using FE software and experimental data. Both single damage and multiple damage cases are simulated in the bridge model with different scenarios. In each scenario, the vibration responses at the considered nodes are recorded and then used to calculate the transmissibility functions. The transmissibility damage indicators are calculated and stored as ANNs inputs. The outputs of the ANNs are the damage type, location and severity. Two machine learning algorithms are used; one for classifying the type and location of damage, whereas the other for finding the severity of damage. The measurements of the Nam O bridge, a truss railway bridge in Vietnam, is used to illustrate the method. The proposed method not only can distinguish the damage type, but also it can accurately identify damage level.

**Keywords:** transmissibility; machine learning algorithm; Artificial Neural Networks (ANNs); Structural Health Monitoring (SHM); large-scale truss bridge

## 1. Introduction

After the completion of a bridge, the three main types of measurement taken during bridge management phase are (1) inspection, (2) assessment and (3) maintenance and repair. With prediction intervals time, the inspections are planned and reduplicated. Visual inspections are normally used, testing and measurements also can be included. An assessment is only carried out whenever it is required. The good assessment can predict the earliest possible time of the damage, then maintenance and repair can be considered. Any change affecting the bridge's performance is considered as damage. Damage includes the change of material and geometric properties, system connectivity, and boundary conditions. Structural health monitoring (SHM) is the process of implementing a damage identification strategy for a structure. Analyzing damage-sensitive

features can determine the current state of system health. These features are extracted from periodically spaced measurements taken over time of the structure or mechanical system. SHM plays a crucial role in increasing the lifespan, boosting operational efficiency, and reducing maintenance costs of the structure. The challenge for SHM is that damage may not crucially affect the lower-frequency global responses, which are usually considered during the system operation. SHM of real civil structures, outside laboratory conditions, is also a challenge. Advanced statistical algorithms need to address the problem that distinguishes damage effects from environmental influences and from damage events (Wahab and De Roeck 1997, Peeters *et al.* 2001). The Switzerland pre-stressed concrete bridge Z24 was selected for testing in the framework of the BRITE-EURAM project SIMCES (Roeck 2003). Researchers monitored this bridge for almost one year before damaging it. They presented a new approach method using eigen frequency to discover abnormal changes due to damage (Peeters and De Roeck 2001). Many test-setup and damage scenarios were performed in this bridge. From that research, many methods had been proposed to detect damage (Maeck *et al.* 2001, Brincker *et al.* 2002, Wahab and De Roeck 1999). Normally, it is difficult to develop a

\*Corresponding author, Professor,  
E-mail: [magd.abdelwahab@tdtu.edu.vn](mailto:magd.abdelwahab@tdtu.edu.vn)

<sup>a</sup> Ph.D. Student

<sup>b</sup> Professor

statistical model for recognizing characteristics between the undamaged and damaged bridge. Recent years, the number of research related to SHM has increased rapidly (Brownjohn 2006). Many bridges in the world are put in monitoring, such as Tamar suspension bridge in Plymouth, UK (Koo *et al.* 2013), Pioneer Bridge, Singapore (Brownjohn *et al.* 2004), Powder Mill bridge, in Barre, Massachusetts, USA (Sanayei *et al.* 2011), etc.

Damage assessment of bridge structures using vibration-based method has been studied since the early 1980s (Farrar and Worden 2006). Modal properties such as frequency response functions (FRF) (Thyagarajan *et al.* 1998), mode shape curvature (Wahab and De Roeck 1999), stiffness matrix (Maia *et al.* 2003, Yan *et al.* 2007), modal data (Kaveh and Maniat 2015), correlation and cross-correlation coefficients (Nguyen *et al.* 2019b) are usually used to identify damage in bridge structures. However, these properties are very sensitive to the environment and operating condition of the bridge. Applying these methods for small localized damage areas faces challenges (Cruz and Salgado 2009). Three new parameters including kurtosis, skewness of signals, and statistical density function are proposed for evaluating crack defects (Nguyen *et al.* 2019c). On the other hand, the advantages of transmissibility in detecting damage are remarked in many research works (Johnson and Adams 2002, Devriendt and Guillaume 2008). The response ratio between two degrees of freedom is described as the transmissibility function. Local damage, which affects the local responses between these degrees of freedom, is expected to be more sensitive to transmissibility than FRF. The damage index based on changes in transmissibility function between undamaged and damage structure is normally used to detect damage. Maia *et al.* (2011) proposed a damage indicator based on correlations of the transmissibility functions and the modal assurance criterion (MAC) in modal analysis. These researchers are in the research team of Maia at IST in Porto (Sampaio *et al.* 2001) and focus on the study of using transmissibility functions to detect and locate damage. Zhou *et al.* (2017) proposed a new method combining transmissibility, hierarchical clustering analysis, and similarity measure to detect damage. The ten-floors structure simulated results and the free-free beam laboratory tests were used to prove the good performance of transmissibility in detecting damage. Transmissibility has been studied to explore structural damage in many research provided by Zhou *et al.* (Zhou *et al.* 2015, 2018, Zhou and Wahab 2016, Zhou 2015). The more recent review on the application of transmissibility-based system identification for SHM was provided in Ref. (Yan *et al.* 2019). This paper is categorized as global, local transmissibility functions, and limits the usage of several methodologies to the following principal features: model updating, modal analysis, and damage detection.

The vibration responses of the bridge under excitation could be used to identify the bridge parameters. The recent developments in vibration measurement instruments and analysis computing technology support this (Deraemaeker *et al.* 2010). Most of the new improvements in the field of SHM has a high contribution from machine learning

technology. ANNs are among the most widely used machine learning techniques and has been trained to discover, localize, and quantify damage in bridge structures. A method of identifying damage through the evaluation of response data from an instrumented bridge proposed in Ref. (Weinstein *et al.* 2018). Lee *et al.* (2005) was used to assess damage of multiple-girder simply supported bridges by using the input of the neural networks as the ratios of the mode shape components between damaged and undamaged scenarios. Mehrjoo *et al.* (2008) presented a method using a back-propagation based neural network for estimating the damage intensities of truss bridge joints. ANNs worked well for assessing the damage in a simply supported beam (Nguyen *et al.* 2018). Vibration-based damage method are based on the principle that can change both the physical properties and dynamic properties. These changes can be used as input for ANNs and the output is the prediction of damage, location, and severity in structures. Sahin and Sheno (2003). In the last 10 years, many researchers used natural frequencies and mode shape curvatures as inputs for ANNs (Hakim and Razak 2014). FRF data was applied to present the healthy conditions of each member in a three-story building and used as the input of ANNs (Wu *et al.* 1992). The measured FRF data reduced via principal component project was handled as the ANNs input variable alternatively of raw FRF (Zang and Imregun 2001). The results showed that the trained ANNs could distinguish between intact and damaged states with a high degree of accuracy. As discussed above, transmissibility is proved to be more sensitive with local damage than FRF. Therefore, in this paper, a novel method that makes use of transmissibility damage indexes as input data of ANNs is proposed. Using transmissibility combined with machine learning has been done before by some authors. Meruane (2015) used transmissibility information to identify anti-resonant frequencies. The changes in the anti-resonant frequencies with respect to the intact were used as the input of ANNs, which could locate and quantify the structural damage. Zhou and Abdel Wahab (2017) used the indicators taken from the transmissibility function as input and then predicted the damage. Nguyen *et al.* (2019a) succeeded in detecting the location and severity of damage in a multiply girders bridge using transmissibility and ANNs. A new approach method is proposed in this paper and makes use of the input parameters calculated from the transmissibility function. The network not only can predict the existence of damage but also can classify the damage types and identify the location of the damage. In this paper, a new application to a large-scale truss bridge, i.e. the Nam O bridge, is considered as a case study to illustrate the proposed method. The results show that the proposed method is successful in assessing large-scale truss bridge damage for most simulated damage scenarios.

This paper has four main sections. The first section is the introduction section. In the second section, we recall some definitions of machine learning, ANNs, and transmissibility. Some proposed ANNs and proposed procedure for detecting damage in a truss bridge are introduced. In the third section, the Nam O bridge is introduced as a case study. The results of the proposed

method are presented. Finally, in the last section, some main conclusions are summarized.

## 2. Methodology

### 2.1 Machine learning algorithm

The scientific study of algorithms and analytical models that can be learned from experience to improve its performance, without human intervention is called Machine Learning (ML). ‘‘Training data’’ is a mathematical model of sample data built by machine learning algorithms. Supervised learning, semi-supervised learning, and unsupervised learning are three main categories of the machine learning algorithm. Supervised learning algorithms using a collection of data carry both the inputs and the desired outputs to create a mathematical model. Semi-supervised learning algorithms work with half-done training data, where a part of the sample inputs does not have desired outputs. In unsupervised learning algorithms, the training data only contains the inputs and no desired outputs. In this paper, we use classification and regression algorithms, which are types of supervised learning. The first task is called classification, which includes designating input originals to one of the discrete classes. These classes are the number and location of damages in the bridge. The second task, which we mention as regression, is treated with foretelling the severity of the damage.

#### 2.1.1 Artificial Neural Networks (ANNs)

ANNs were designed to contain a family of mathematical models. Inverse, ANNs can be used for solving math (Anitescu *et al.* 2019). The structure of biological neural networks is the source of ANNs creation. Pattern recognition problem, as we have indicated, must find out the non-linear mappings between a collection of input and output variables. The mapping is therefore created as mathematical functions. Adjustable parameters in these functions are resolved from training data. The output variables of ANNs is the results of the combination function between the bias function or hidden functions  $z_j(x)$  with weight parameters  $\omega_{kj}$

$$y_k(x) = \sum \omega_{kj} z_j(x) \quad (1)$$

Where  $y_k(x)$  represents the output variables.

The neural network has a number of the layers. The first layer is the input layer and the last layer is the output layer. The hidden layers are between these two layers. Each layer have a series of nodes. Each node represents one neuron. The number of hidden layers and the number of nodes are decided based on the relationship between input and output data and on the number of nodes in the input and output layers. The goal is to train the network maps new inputs correctly and not to over-fit the data. The ANNs structure is illustrated in Fig. 1.

If the network has one hidden layer, the bias functions themselves contain adaptive parameters and are expressed by

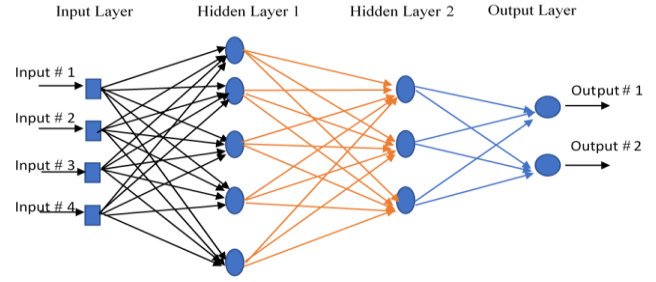


Fig. 1 A neural networks structure

$$z_j(x) = g \left( \sum \omega_{ji} x_i + b_j \right) \quad (2)$$

Where  $\omega_{ji}$  and  $b_j$  are the weight and bias parameters and  $x_i$  represents the input variables. If the network has more than one hidden layer, the procedure will continue with more hidden functions. The function  $g(\cdot)$  is called an activation function. Many kinds of activation function can be examined to optimize the network parameters. The most common used functions are expressed below.

$$g(a) = \tan^{-1}(a) \quad g(a) = \frac{1}{1 + e^{-a}} \quad (3)$$

$$g(a) = \tanh(a) = \frac{e^{2a} - 1}{e^{2a} + 1}$$

#### 2.1.2 Pattern classification

The ANNs considered above for classifying the types and locations of damages was designed to take the input data and to assign it to one of those classes, e.g., Damage Case 1 (DC1), Damage Case 2 (DC2), Damage Case 3 (DC3), etc. We can present the outcome of the classification in terms of variable  $y_k$  (output variable), where  $k$  is the number of class. If the sample represents DC1, then  $y_1$  takes the value 1, whereas  $y_2$  and  $y_3$  take the value 0. Similarly, if the sample represents DC2 then  $y_2$  takes the value 1, whereas  $y_1$  and  $y_3$  take the value 0.

Consider the problem of two classes’ prediction between Damage Case 1 (DC1) and other Damage Cases (DC#). The two classes are labeled as DC1 (Positive) and DC# (Negative). Fig. 2 illustrates the Probability Density Functions of this case. For each threshold, there are four achievable results from a binary classifier. It is named a true positive (TP) if the actual class is DC1 and the results from the prediction is also DC1. It is named a false positive (FP),

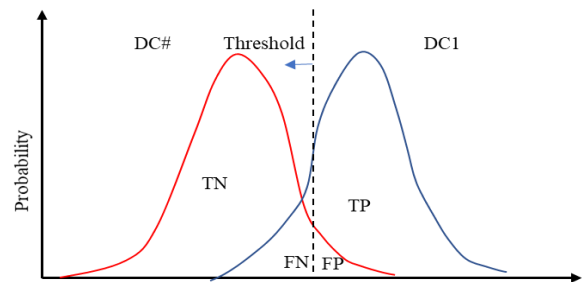


Fig. 2 Distributions from the class DC1 and other classes DC#

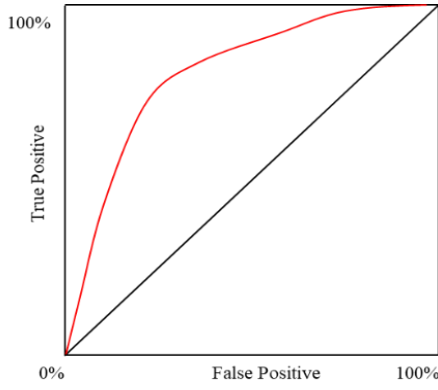


Fig. 3 The receiver operating characteristic (ROC) curve

Table 1 The confusion matrix for classifying DC1 and DC#

Outcome	Observed		
	Positive	Negative	
Positive	True positive ( <i>TP</i> )	False positive ( <i>FP</i> )	<i>PPV</i> <i>FDR</i>
	False negative ( <i>FN</i> )	True negative ( <i>TN</i> )	<i>FOR</i> <i>NPV</i>
	<i>TPR</i>	<i>FPR</i>	
	<i>FNR</i>	<i>TNR</i>	<i>ACC</i>

if the actual class is DC# and the results from the prediction is also DC1. For a negative results, there can be either true negative (*TN*) if prediction class the same as actual class as DC# or false negative.

Both TP and FP are zero if the threshold is located at the right of the null distribution and DC1 is not detected. The area below the null distribution extends if the threshold moves to the left. The four outcomes can be formulated in a confusion matrix, as show in Table 1, where the correct classifications are presented by numbers along the major diagonal.

Where:

$$PPV: \text{Positive Predictive value; } PPV = \frac{TP}{TP+FP}$$

$$FDR: \text{False Discovery Rate; } FDR = \frac{FP}{TP+FP}$$

$$FOR: \text{False omission rate; } FOR = \frac{FN}{FN+TN}$$

$$NPV: \text{Negative Predictive value } NPV = \frac{TN}{FN+TN}$$

$$TPR: \text{True Positive Rate; } TPR = \frac{TP}{TP+FN}$$

$$FNR: \text{False Negative Rate; } FNR = \frac{FN}{TP+FN}$$

$$FPR: \text{False Positive Rate; } FPR = \frac{FP}{FP+TN}$$

$$TNR: \text{True Negative Rate; } TNR = \frac{TN}{FP+TN}$$

$$ACC: \text{Accuracy; } ACC = \frac{TP+TN}{TP+FN+FP+TN}$$

Another general and graphical way to review the achievement of classifiers is by using receiver operating characteristic (ROC) curves (Fawcett 2004). Fig. 3 plots the ROC curve, where the horizontal axis is the false positive rate (*FPR*) versus the vertical axis is the true positive rate

(*TPR*). The *TPR* and *FPR* are often called as sensitive and specificity, respectively. The ROC space is divided into two parts by the diagonal line. If the classifier understands the classes, the points in ROC is in the upper left triangle. The practical way to see the accuracy of the method is to analyze the area under the curve; i.e., the value 1 for perfection and value 0.5 for worthless.

### 2.1.3 Regression analysis

Assigning new inputs to one of the discrete classes is the main task of classification problems. However, if there are many other pattern recognition tasks, we shall refer to as regression problems, in which the outputs represent the value of continuous variables. In this paper, the severity of the damage in one element varies from 10% to 60%. The output of the network should be continuous variables corresponding to the target output, i.e. the severity of damage.

Linear regression is the simplest form of regression. Our task is to find the best weight parameters and active function providing the best fit to our data. One way to measure the fit is measuring the mean square error (*mse*) as defined in Eq. (4), where  $y_k$  represents the network outputs  $y$  and  $t_k$  represents the desired outputs. In order to find the best fit, we must minimize *mse*.

$$mse = \frac{1}{N} \sum_{k=1}^N (e_i)^2 = \frac{1}{N} \sum_{k=1}^N (t_k - y_k)^2 \quad (4)$$

## 2.2 ANNs approach for structural damage assessment

### 2.2.1 Structural damage

Steel bridges are often selected in a case where the live load is large or the effective span is long, as in railway bridges. Steel truss bridges have higher adaptability than other kinds of bridges. For example, when one truss member is damaged, it's not difficult to replace it by a new one. There are various types of damages in steel truss bridges including damage in joints (Mehrjoo *et al.* 2008) and main members (Lee *et al.* 2005, Barai and Pandey 1997, Yeung and Smith 2005). Most metals exist in the form of oxides. Therefore, corrosion may appear on steel material in the atmosphere, water and seawater. The appearance of corrosion in a truss member reduces its stiffness. Defining  $k_i$  as the stiffness reduction in the truss member  $i$ , the undamaged truss and completely damaged truss are represented by  $k_i = 0$  and  $k_i = 1$ , respectively. Eq. (5) expresses this definition, where  $K_i$  and  $K_i^d$  are the undamaged and damage stiffness of the  $i$  element, respectively.

$$K_i^d = K_i(1 - k_i) \quad (5)$$

### 2.2.2 Transmissibility damage index as input data

Consider the structural vibration, the transmissibility  $T_{i,j}(\omega)$  is described simply as the ratio between two responses in the frequency domain when an excitation force is applied, i.e.

$$T_{i,j}(\omega) = \frac{X_i(\omega)}{X_j(\omega)} \quad (6)$$

Where:  $X_i(\omega)$  and  $X_j(\omega)$  are the responses at location  $i$  and  $j$  in the frequency domain, respectively.

When used for detecting damage, the transmissibility is more effective if restricted to specific frequency bands (Worden *et al.* 2003). The indicator  $TI_{i,j}$  is defined in Eq. (7) to enhance the sensitivity of transmissibility associative with the structural deterioration or damages.

$$TI_{i,j} = \int_{f_{min}}^{f_{max}} T_{i,j} df \quad (7)$$

Where  $f_{min}$  and  $f_{max}$  are the low and high boundary of frequency band.

The indicator  $TI_{i,j}$  of intact bridge at all locations is used to calculate the damage indicator. The damage indicator value is the difference between the transmissibility indicator at all locations of the damaged bridge and intact bridge for a given frequency band.

$$DI_k = \frac{TI_{i,j}^u - TI_{i,j}^d}{TI_{i,j}^u} \quad (8)$$

Where,  $TI_{i,j}^u$  is the transmissibility indicator of the undamaged bridge and  $TI_{i,j}^d$  is the transmissibility indicator of the damaged bridge.

The damage indicator should take the mean value of all measurement times. The damage indicators of all transmissibility functions will be stored and then used as the input data of ANNs.

### 2.2.3 Procedure for damage detection

Step 1: The procedure starts with the sensors setup. For truss bridges, the sensors are placed at the nodes, where the desired mode shapes of the bridge can be measured. The model of the bridge, which is created by using a finite element software, is updated with the help of these data.

Step 2: The displacement response of selected nodes in step 1 is calculated from updated FEM and then transformed to the frequency domain. The load excitation is the moving vehicle, running across the bridge with the constant velocity. The weight of the vehicle is assumed to be constant, too. Several vehicle weights are considered in this step. Random Gaussian noise is added to the simulated responses. Damage indicators are estimated based on transmissibility, Eqs. (6)-(8). This procedure is applied to all considered vehicle weight potential damage locations and severities. Then the damage indicators are stored as input and the damage locations and the severities are stored as the desired output of the ANNs.

Step 3: ANNs training and testing are performed and the best performance ANNs is stored.

Step 4: Implementation for the real bridge (see step 1) is carried out. The sensors are installed in the damaged bridge at the same location at step 1. The displacement response of those sensors is recorded then transformed into the frequency domain. The load excitation should be in the

range of vehicle weight considered in step 2. Damage indicators are estimated based on transmissibility, Eqs. (6)-(8) again. Then all these damage indicators are used as input of the best ANNs created in step 3. The output of this ANNs is the location and the severity of the damage in the bridge.

## 3. Case study

### 3.1 The Nam O bridge

The Nam O bridge is a long-span railway bridge opened in 2011, under the support of the Ho Chi Minh City - Hanoi Line traffic Safety Improvement Project. The Nam O bridge is located at Da Nang city, Vietnam. The bridge across Cu De river, hold the train traffic from the North to the South. The bridge consists of four simply supported spans, with the length of 75 m for each span. The rail track is directly fastened to the stringers of the bridge deck. The view of the bridge from the downstream side is displayed in Fig. 4 while Fig. 5 shows the main structural elements of the bridge. Main structural elements included top chords, bottom chords, verticals, diagonals, portal frames, and stringers. The cross-sectional properties of the truss members are presented in Table 2. The steel material has elastic modulus of  $2.05 \times 10^{11}$  N/m<sup>2</sup>, density of 7850 kg/m<sup>3</sup> and Poisson's ratio of 0.3.

### 3.2 Experimental Measurements and FEM updating

The ambient vibration was performed on the first span from the upstream side of the river. The bridge free



Fig. 4 The Nam O bridge (Tran-Ngoc *et al.* 2018)

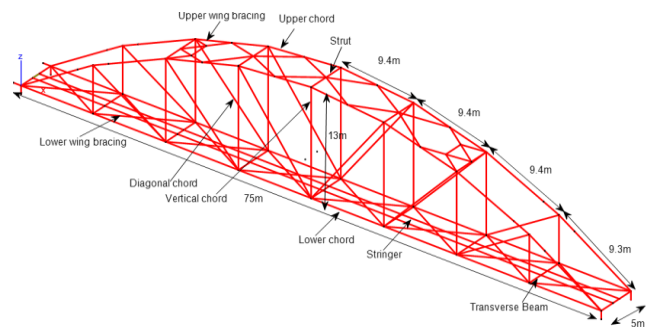


Fig. 5 The Nam O bridge main structural elements (Tran-Ngoc *et al.* 2018)

Table 2 Cross-sectional properties of main structural members

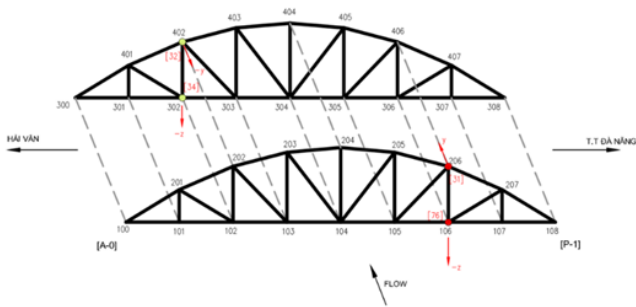
Member		Area $A$ (m <sup>2</sup> )	Moment of inertia $I_z$ (m <sup>4</sup> )	Moment of inertia $I_y$ (m <sup>4</sup> )
Upper chord	Type 1	0.056	$6.70 \times 10^{-04}$	$3.1 \times 10^{-03}$
	Type 2	0.054	$6.46 \times 10^{-04}$	$2.93 \times 10^{-03}$
	Type 3	0.034	$4.30 \times 10^{-04}$	$1.90 \times 10^{-03}$
	Type 4	0.034	$4.3 \times 10^{-04}$	$1.90 \times 10^{-03}$
Lower chord		0.020	$2.10 \times 10^{-04}$	$6.30 \times 10^{-04}$
Vertical chord	Type 1	0.010	$5.49 \times 10^{-05}$	$1.15 \times 10^{-04}$
	Type 2	0.023	$1.60 \times 10^{-04}$	$6.50 \times 10^{-04}$
	Type 3	0.014	$1.24 \times 10^{-04}$	$2.78 \times 10^{-04}$
Diagonal chord	Type 1	0.014	$1.24 \times 10^{-04}$	$2.78 \times 10^{-04}$
	Type 2	0.015	$1.20 \times 10^{-04}$	$3.40 \times 10^{-04}$
	Type 3	0.015	$1.20 \times 10^{-04}$	$4.00 \times 10^{-04}$
Stringer		0.020	$2.07 \times 10^{-04}$	$6.27 \times 10^{-04}$
Transverse beam	Type 1	0.026	$2.03 \times 10^{-04}$	$3.61 \times 10^{-03}$
	Type 2	0.026	$9.25 \times 10^{-04}$	$3.20 \times 10^{-03}$
Strut	Portal Frame	0.053	$6.25 \times 10^{-04}$	$2.80 \times 10^{-03}$
	Type 1	0.020	$1.48 \times 10^{-04}$	$1.86 \times 10^{-03}$
	Type 2	0.022	$1.50 \times 10^{-04}$	$3.20 \times 10^{-03}$
	Type 3	0.021	$1.60 \times 10^{-04}$	$2.00 \times 10^{-03}$
Upper wind bracing	Type 1	0.0036	$8.00 \times 10^{-04}$	$1.09 \times 10^{-05}$
	Type 2	0.0019	$1.90 \times 10^{-06}$	$1.40 \times 10^{-06}$
Lower wind bracing		0.0049	$2.38 \times 10^{-06}$	$4.38 \times 10^{-06}$



Fig. 7 Placement of accelerometers and LDVTs at one node of Nam O bridge

LVDT sensors are set up on the bridge to measure 40 DOFs (Fig. 7). The DOFs in each setup can be found in Fig. 6, where the  $x$ -axis is in the longitudinal direction of the bridge; the  $y$ -axis is in the transverse direction (to the river flow direction) and the  $z$ -axis is in the vertical direction. Nodes 100, 300, 308 and 108 are the location of bearings. Three sensors in  $x$ -axis direction were placed at three nodes 100, 300 and 308. Two sensors along  $y$ -axis were placed at three nodes 100, 300 and no sensor at the fixed node 108. The real bearings operational conditions are updated by using these five sensors. The measurement time was about ten to twenty minutes per setup and the sampling rate was 1651 Hz.

Table 3 shows the summary of the first 10 extracted mode shapes, within the frequency range from 1.45 Hz to 6.05 Hz. In order to solve the model updating problem, these ten modes are enough. The finite element model of



- Setup 1: 106z 206y 302z 402y 101z 103z 301z 303z 305z
- Setup 2: 106z 206y 302z 402y 102z 104z 107z 304z 306z 307z
- Setup 3: 106z 206y 302z 402y 102y 103y 104y 304y 306y 307y
- Setup 4: 106z 206y 302z 402y 101y 105y 107y 301y 303y 305y
- Setup 5: 106z 206y 302z 402y 102y 103y 104y 304y 306y 307y
- Setup 6: 106z 206y 302z 402y 100x 100y 300y 300x 308x
- Setup 7: 106z 206y 302z 402y 403y 404y 405y 406y
- Setup 8: 106z 206y 302z 402y 201y 207y 401y 407y

Fig. 6 The measurement grid, the position of reference sensors and setups

vibration after train passage was measured. Eight setups were carried out with four fixed reference sensors, distributed on the two-bay of the span at both lower node and upper one as shown in Fig. 6. Accelerometers and

Table 3 The first ten natural frequencies from FEM updating compared to the measurement

Mode No.	FEM updating – PSO (Hz)	Measurement (Hz)	Differences (%)	Mode type
1	1.45	1.45	0	Transverse mode
2	3.10	3.11	0.3	Transverse mode
3	3.27	3.28	0.3	Lateral torsion
4	4.66	4.62	0.8	First bending
5	6.55	6.05	7.6	Local mode of the two bays at ends
6	7.15	7.12	0.4	Local mode of the two bays at ends
7	7.33	7.30	0.5	Transverse mode
8	8.10	7.46	8.57	Transverse mode
9	9.00	8.29	7.94	Combination mode
10	9.57	8.89	7.10	Second vertical bending

Nam O Bridge was built based on the geometry from the as-built drawings using the MATLAB toolbox StaBil (Dooms *et al.* 2010). The FE model includes 137 nodes and 227 beam elements. The elements are Timoshenko beams, which estimate the impacts of shear-deformation. Each node of elements includes 6 degrees of freedom consisting of translations around the  $x$ ,  $y$ , and  $z$  axes and rotations in the  $x$ ,  $y$ , and  $z$  axis. Rotational springs were used to model the connections between truss members and the springs were employed to model the bearings. Tran-Ngoc *et al.* (2018) used the Particle Swarm Optimization algorithm updating the model so that the frequencies from the FE model and from measurement match. Considering Table 3, the results from modes 1 to 3 perfectly match and the differences between FEM and measurement for other natural frequencies are less than 10%. More details about the measurement, FEM bridge, and model updating can be found in Ref. (Tran-Ngoc *et al.* 2018).

### 3.3 The proposed ANNs method

In the Nam O bridge, each span has got two main trusses as shown in Fig. 6. Each main truss has 29 elements and 16 nodes, which have been labeled. In the experiment, eight setups were used to measure 40 DOFs. Therefore, in the first step of detecting damage, we proposed finding the displacement responses of these DOFs for all damage scenarios. Damage in all lower chords was taken into account in this paper. Three cases of damage including damage in single element (DC1), damage in two elements (DC2) and damage in three elements (DC3) were introduced. We reduced the stiffness of each element to reflect the damage severity. In DC1, the stiffness is reduced from 10% to 60% with an interval of 1%. In DC2, the stiffness is reduced from 1% to 60% with an interval of 5% for both elements and we use the same reduction and interval for three elements in DC3. We use 16 single damaged elements from S1 to S16 in DC1, so that we have 800 sampling data. Six cases of DC2; from M1 to M6 are introduced and 864 sampling data are restored. Only one case of 3 elements damage (M7) is considered, and then 1728 scenarios and sampling data are restored. Table 4 shows the damaged elements in the three cases, where one element is denoted by two nodes, for example element 100-101 connects node 100 and 101. All the damage scenarios are simulated using FEM in Matlab.

As Nam O bridge is a railway bridge, a locomotive is proposed as an excitation force. Three locomotive weights (35 tons, 33 tons, and 30 tons) are used to get the data for training the network. This locomotive has three axels and the distance between the two axels is 1.5 m. The weight is divided equally on the three axels. The displacement responses at 40 DOFs are calculated based on FE results. The axle load is modelled using a forced matrix in the finite element model. When the locomotive runs on the bridge, the force is transmitted to the longitudinal beam, and then transmitted to the truss joints in the direction of DOF. Gaussian noise is considered in the numerical displacement response. The signal to noise ratio ranges from 70 dB to 50 dB.

Table 4 Details of damage elements in three damaged cases

Mode No.	FEM updating – PSO (Hz)	Measurement (Hz)	Differences (%)	Mode type
1	1.45	1.45	0	Transverse mode
2	3.10	3.11	0.3	Transverse mode
3	3.27	3.28	0.3	Lateral torsion
4	4.66	4.62	0.8	First bending
5	6.55	6.05	7.6	Local mode of the two bays at ends
6	7.15	7.12	0.4	Local mode of the two bays at ends
7	7.33	7.30	0.5	Transverse mode
8	8.10	7.46	8.57	Transverse mode
9	9.00	8.29	7.94	Combination mode
10	9.57	8.89	7.10	Second vertical bending

There are four fixed sensors in the measurements. These reference sensors are located at the points of significant modal displacements of many modes that measure 4 DOFs 106z, 206y, 302z, 402y. To calculate the transmissibility indicators, these 4 DOFs are used as reference joints. The displacement responses are transform to frequency domain to calculate the transmissibility. Those transmissibility functions are:

Reference node 106 in z direction:

$$T_{100,106}, T_{101,106}, T_{102,106}, T_{103,106}, T_{104,106}, T_{107,106}.$$

Reference node 206 in y direction:

$$T_{100,206}, T_{101,206}, T_{102,206}, T_{103,206}, T_{104,206}, T_{105,206}, T_{201,206}, T_{207,206}.$$

Reference node 302 in z direction:

$$T_{301,302}, T_{303,302}, T_{304,302}, T_{305,302}, T_{306,302}, T_{307,302}.$$

Reference node 402 in y direction:

$$T_{300,402}, T_{301,402}, T_{303,402}, T_{304,402}, T_{305,402}, T_{306,402}, T_{307,402}, T_{401,402}, T_{403,402}, T_{404,402}, T_{405,402}, T_{406,402}, T_{407,402}.$$

In x direction:  $T_{100,308}$ .

In total, from 40 DOFs, 34 transmissibility functions  $T_{i,j}(\omega)$  are calculated using Eq. (6). The transmissibility indicators are then calculated using Eq. (7) at frequency band from 0.8 Hz to 2.5 Hz. Finally, 34 damage indicators DI are determined using Eq. (8) and restored as input of ANNs. This procedure is repeated for all scenarios.

The combination of two machine learning algorithms are proposed for detecting damage in Nam O bridge. The ANNs using pattern recognition algorithm is trained to classify the damage. The ANNs using regression algorithm is trained to find the severity of the damage. The classification problems can be solved by using a two-layer feed-forward network. From the input data and desired output, the network divides data into training, validation,

and testing sets, which define the network architecture and train the network. The three classes used are DC1, DC2, and DC3. We choose the network with two hidden layers. Hidden layer 1 has 350 neurons and hidden layer 2 has 50 neurons. The network architecture is shown in Fig. 8. This network then will be trained and validated using *trainscg* (Scaled conjugate gradient back propagation) training function in Matlab, *cross entropy* are used as loss function. After classifying the damage cases, the severity of the damage can be found by using the second machine learning algorithm. The structure of this ANNs is shown in Fig. 9, Figs. 10 and 11 for DC1, DC2 and DC3, respectively. The number of hidden layers and neurons should be taken into account (Guo *et al.* 2019). In this work, the structure of ANNs is chosen by trial and error. These regression networks were trained by using mean square error (*mse*) performance and Levenberg-Marquardt training algorithm. The results of these networks working will be shown in the next section. Fig. 12 shows the procedure to create ANNs from the numerical model data set. These networks can be stored and used for any new cases.

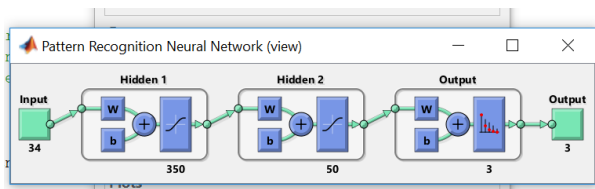


Fig. 8 The structure of the pattern recognition neural network

### 3.4 Results and discussion

#### 3.4.1 Intact bridge

The transmissibility function is calculated following the procedure discussed in Section 3.3. These transmissibility functions are taken from the simulated responses of the considered DOFs and locomotive weight. Fig. 13 shows the function  $T_{100,106}$  before and after using the GRNN function for approximation. The load excitation is the 35-ton locomotive. The peaks and the valleys of these two functions appear at the same frequencies instead of the oscillation of the functions got from the numerical model. This function is oscillating because of the numerical response and the moving load being calculated every 0.005 s, instead of being a continuous variable. GRNN are single-pass associate memory feed-forward type ANNs suggested by Specht (1991). Using this method, we can calculate 34 transmissibility functions described above for the intact bridge. Only three functions  $T_{100,106}$ ,  $T_{102,106}$ ,  $T_{104,106}$  are plotted in Fig. 14. Other functions have similar shape.

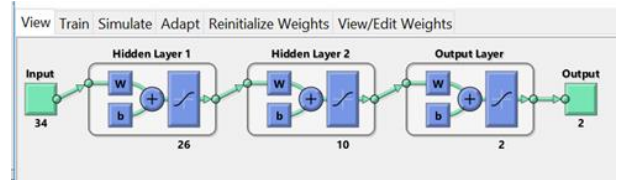


Fig. 10 The structure of the regression neural network for DC2

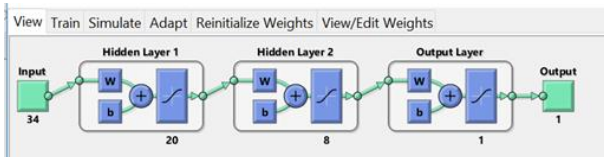


Fig. 9 The structure of the regression neural network for DC1

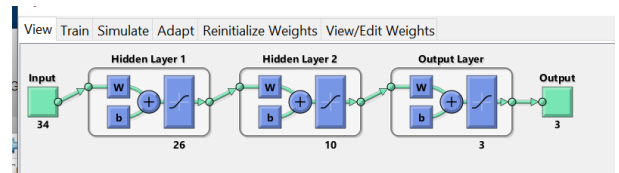


Fig. 11 The structure of the regression neural network for DC3

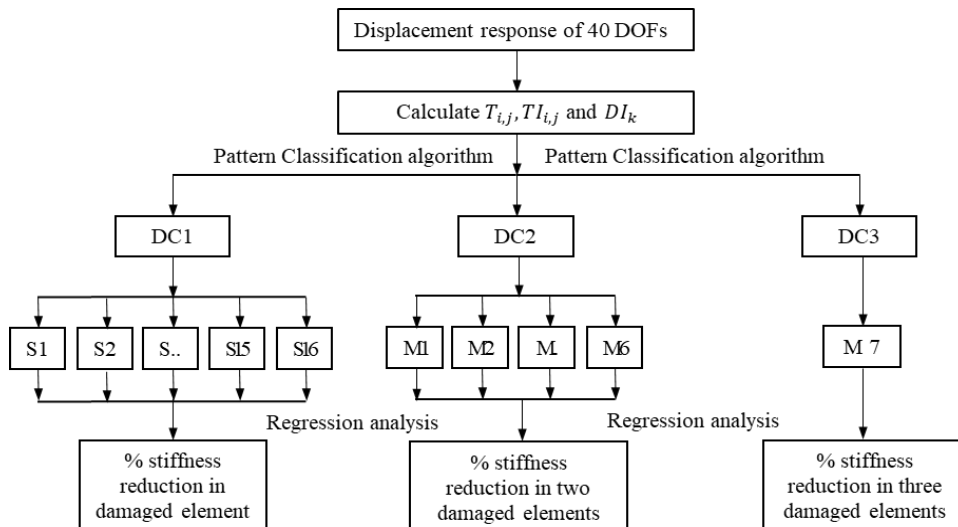


Fig. 12 The procedure for create ANNs used in damage detection of the Nam O Bridge

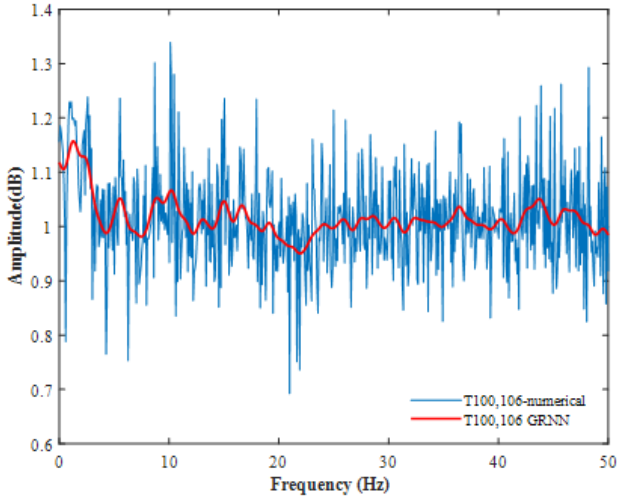


Fig. 13  $T_{100,106}$  calculated from numerical model and GRNN approximation function, excited by 35 tons locomotive

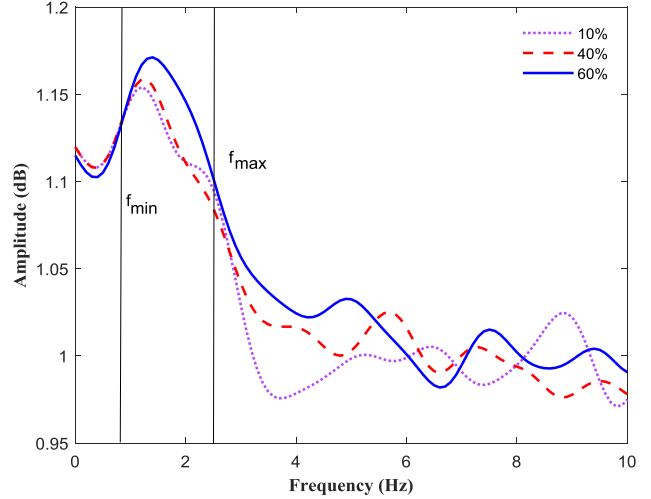


Fig. 15 Transmissibility functions  $T_{102,106}$ , for the case of damage at element 307-308

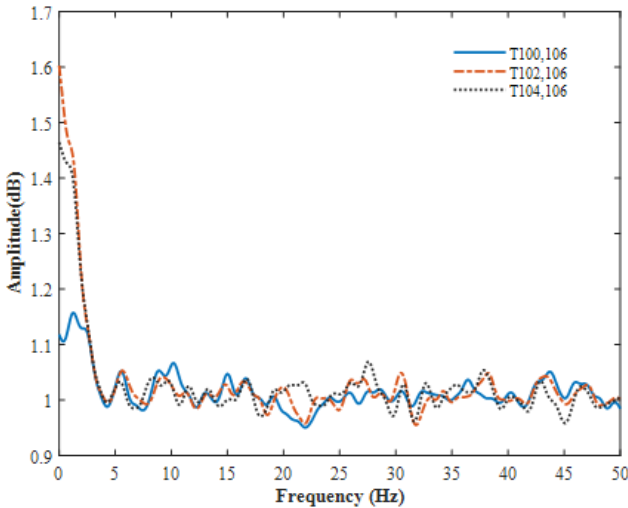
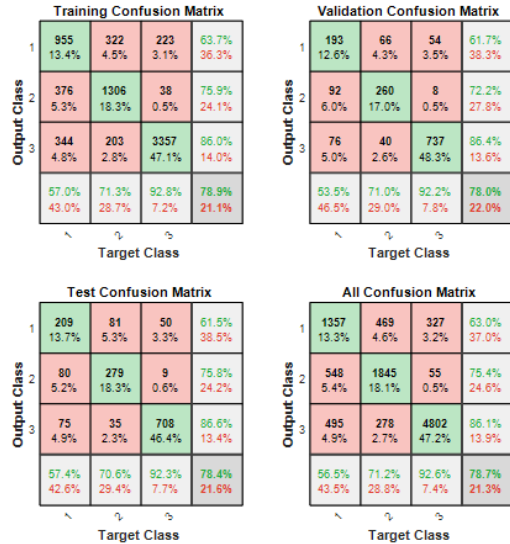
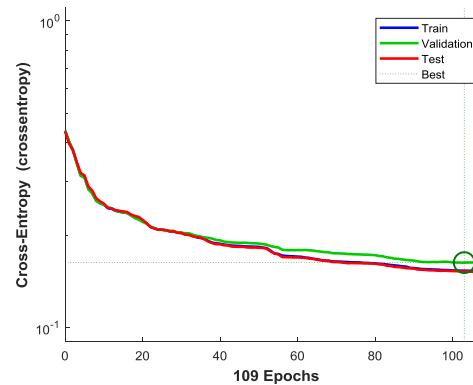


Fig. 14 Transmissibility functions of intact bridge excited by 35 tons locomotive



(a) Confusion matrix



(b) Performance progress

Fig. 16 DC1, DC2, DC3 classification results

### 3.4.2 Damaged bridge

As discussed in section 3.3, 34 transmissibility functions are calculated and the damage indicators (DI's) are determined based on the TI indicator. Fig. 15 shows the transmissibility functions  $T_{102,106}$ . The percentages, 10%, 40%, and 60%, are the stiffness reduction of the element 307-308. The first peak is chosen for the calculation of TI, frequency range from 0.8 Hz to 2.5 Hz. We can see that when the severity of the damage increases, the transmissibility function changes and then increases.

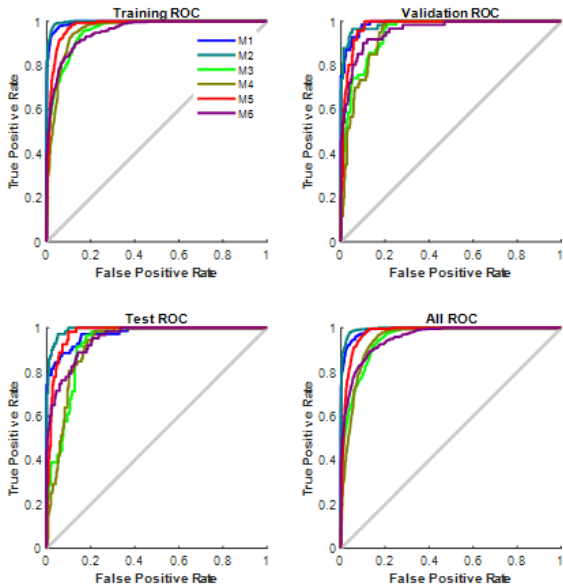
There are three cases of damage DC1, DC2, and DC3 as discussed above. In the first task, we use ANNs shown in Fig. 8 to classify these 3 damage cases. There is 2400 samples of DC1, 2592 samples of DC2 and 5184 samples of DC3. These data are divided into 3 parts: 70% for training, 15% for validation and 15% for a test. In the confusion matrix shown in Fig. 16(a), the numbers 1, 2, 3 means DC1, DC2 and DC3, respectively. We see that 57.0% of the times

in the training confusion matrix, 53.5% of the times in the validation confusion matrix, 57.4% of the times in the test confusion matrix, classifies DC1 correctly. The performance progress in Fig. 16(b) indicates that the

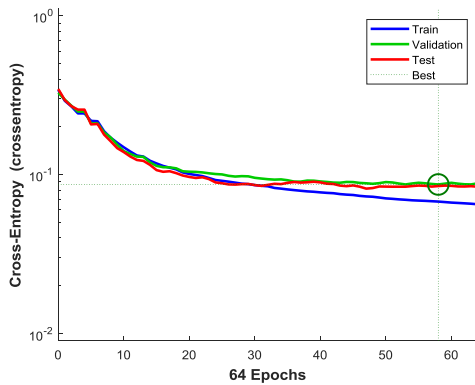
iteration at which the validation performance reached a minimum is epoch 104. The training progresses well, the cross-entropy loss decreases when the number of epoch increases. Similarly, ANN classifies DC2 correctly for 71.3% of the times in the training confusion matrix, 71.0% of the times in the validation confusion matrix, 70.6 % of the times in the test confusion matrix. The DC3 has the biggest samples and the highest percentage of correct classification, too. 92.8% of the times in the training confusion matrix, 92.2% of the times in the validation confusion matrix, 92.3 % of the times in the test confusion matrix are classified correct. In all cases, 78.7% are correctly classified. As discussed above, DC1 have 16 cases of damage, from S1 to S16, DC2 have 8 cases of damage from M1 to M6. Pattern networks are used again for classification. Fig. 17 shows the ROC curves and performance progress from M1 to M6. Fig. 18(a) draws some ROC curves, each corresponds to different scenario S1 to S16. The area under the ROC curve, which is close to 1, means that the method's accuracy is high. The correct percentage, in this case, is 80.0% of 2598 samples being classified correctly in DC2 and the correct percentage for DC1 is 77.8%. The figures of performance progress indicate

a very similar trend between validation and test data (Figs. 17(b) and 18(b)). The overfitting does not occur in this case. These results proved that ANNs are successful in finding out the type and the location of the damage.

To find out the damage severity, we use regression networks as shown in Fig. 19. The output of this network is the severity of the damage. For DC1, the input of the network is the 34 transmissibility indicators and the target of the network is the percentage of the stiffness reduction in the damaged element. For DC2, there are two targets of the network that are the percentages of the stiffness reduction at the two damaged elements. Similarly, for DC3, there are three targets corresponding to 3 damaged elements. Fig. 19(a) shows a relationship between the outputs of the network and the target in S1 scenario. There are four plots corresponding to the training data sample, validation data sample, testing data sample, and all datasets. The dashed line in each plot presents the perfect line  $outputs = targets$ .  $R$ -value is the correlation coefficient between the outputs and targets. It is a measure of how well the variation in the output is explained by the targets.  $R = 1$  indicates that the network outputs are perfectly fit the targets. All four  $R$ -values in Fig. 19(a) are approximately 0.9 indicating a nearly perfect fit. The variation of mean square error versus the different number of epochs was plotted in Fig. 19(b).

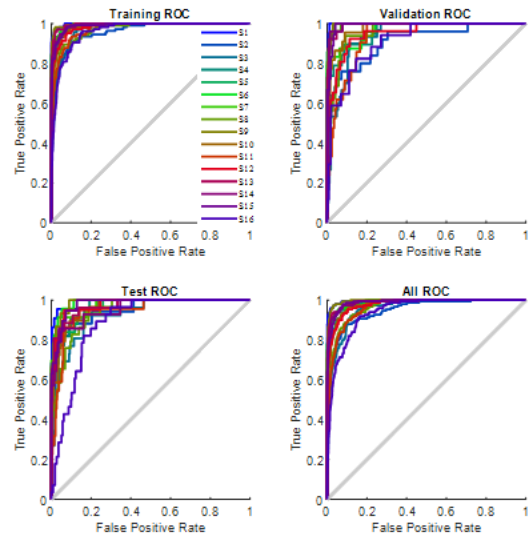


(a) ROC curves

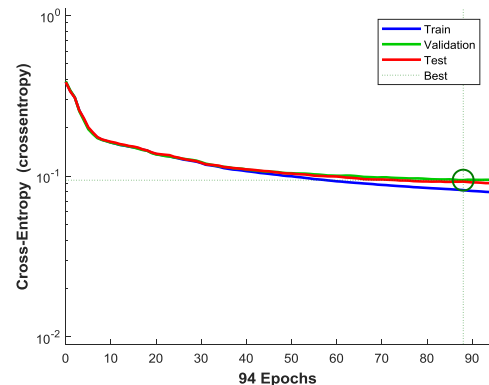


(b) Performance progress

Fig. 17 DC2 classification results

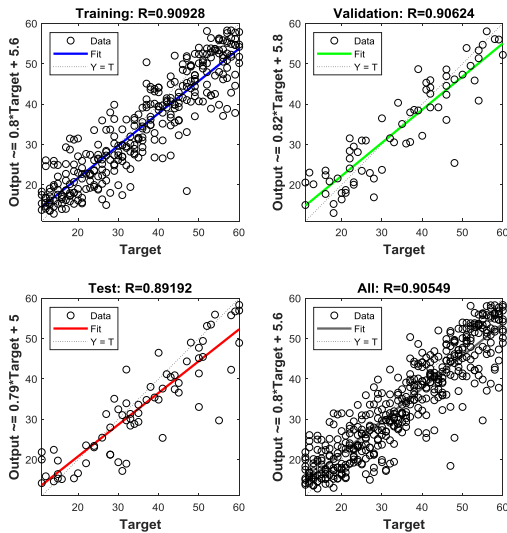


(a) ROC curves

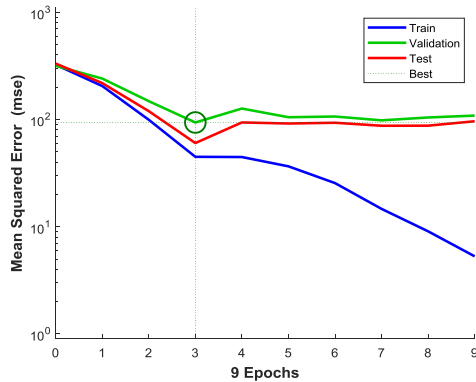


(b) Performance progress

Fig. 18 DC1 classification results



(a) Regression analyses



(b) Performance progress

Fig. 19 S1 scenario regression analysis results

Table 5 R-value of the network

Scenario	S1	S2	S3	S4	S5	S6
R-value	0.905	0.918	0.852	0.938	0.940	0.981
Scenario	S7	S8	S9	S10	S11	S12
R-value	0.983	0.944	0.981	0.953	0.85	0.968
Scenario	S13	S14	S15	S16	M1	M2
R-value	0.980	0.935	0.965	0.90	0.867	0.86
Scenario	M3	M4	M5	M6	M7	
R-value	0.901	0.956	0.871	0.942	0.773	

The *mse* decreases with the increase in the number of epochs. The best performance is in epoch 3. The training continued for six more iterations before it stopped. The validation and test curves are similar. No problem occurred in the training progress.

Table 5 shows the *R*-value of the networks for all damaged scenarios. M7 is the most complicated scenario with 3 damaged elements having the lowest *R*-value. All the *R*-value is larger than 0.75, most of them larger than 0.90. This proves that ANNs are successful in finding out the severity of the damage in each damaged element. This ANNs then can be stored and used for any new case.

Therefore, we can conclude that using machine learning algorithms of the different types can help us in assessing the damage of Nam O bridge.

#### 4. Conclusions

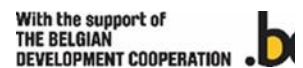
A novel methodology has been here proposed, based on the machine learning algorithm, to provide an approach for assessing damage in a truss bridge with acceptable accuracy. The transmissibility damage indicator was calculated from an updated FE model of the bridge and then used as the input data of ANNs. There are many kinds of machine learning algorithms that can be used depending on the desired purpose. In this paper, the author proposes using a combination of two algorithms. The Pattern Recognition algorithm was used to classify the type and location of damages. The Regression algorithm was applied to find the damage severities. First, the FEM is used to train the network. Then, the user provides the input data (the damage indicators calculated from experiments). The results indicated that the ANNs could distinguish the damage appearing at one element, two elements or three elements and found out the severity of the damages.

Transmissibility and machine learning algorithm are two methods that only based on output responses only. Therefore, the combination of these two methods is very interesting. It is important to note that the proposed method needs a large number of measurement points. The more DOFs we consider, the more accurate the networks. The actual technology permits this to occur. The vibration response of the bridge can be measured at many points. This shows a promising future in real applications of SHM.

Several excitation loads are used to train the network in this research. The results are still good. This proved that if the number of samples is big enough, the real excitation load doesn't have to be the same as the load used for the numerical simulations. But the real excitation load should be in the range of trained excitation load. This research doesn't consider the effect of temperature, the roughness of the bridge slab, humidity, wind load, etc. But ANNs work very well with big data. All of the conditions that influence the response of the bridge can be considered in the input of the network. Considering these effects will be the subject of our future research.

#### Acknowledgments

The authors acknowledge the financial support of VLIR-UOS TEAM Project, VN2018TEA479A103, 'Damage assessment tools for Structural Health Monitoring of Vietnamese infrastructures', funded by the Flemish Government



## References

- Anitescu, C., Atroshchenko, E., Alajlan, N. and Rabczuk, T. (2019), "Artificial neural network methods for the solution of second order boundary value problems", *Comput. Mater. Continua*, **59**(1), 345-359. <https://doi.org/10.32604/cmc.2019.06641>
- Barai, S. and Pandey, P. (1997), "Time-delay neural networks in damage detection of railway bridges", *Adv. Eng. Software*, **28**(1), 1-10. [https://doi.org/10.1016/S0965-9978\(96\)00038-5](https://doi.org/10.1016/S0965-9978(96)00038-5)
- Brincker, R., Andersen, P. and Zhang, L. (2002), "Modal identification and damage detection on a concrete highway bridge by frequency domain decomposition", *The Structural Engineering World Conference: SEWC*. Citeseer.
- Brownjohn, J.M. (2006), "Structural health monitoring of civil infrastructure", *Philosophical Transactions of the Royal Society A: Mathematical, Physical and Engineering Sciences*, **365**(1851), 589-622. <https://doi.org/10.1098/rsta.2006.1925>
- Brownjohn, J., Rizos, C., Tan, G.-H. and Pan, T.-C. (2004), "Real-time long-term monitoring and static and dynamic displacements of an office tower, combining RTK GPS and accelerometer data".
- Cruz, P.J. and Salgado, R. (2009), "Performance of vibration-based damage detection methods in bridges", *Comput.-Aid. Civil Infrastruct. Eng.*, **24**(1), 62-79. <https://doi.org/10.1111/j.1467-8667.2008.00546.x>
- Deraemaeker, A., Preumont, A., Reynders, E., De Roeck, G., Kullaa, J., Lamsa, V., Worden, K., Manson, G., Barthorpe, R. and Papatheou, E. (2010), "Vibration-based structural health monitoring using large sensor networks", *Smart Struct. Syst., Int. J.*, **6**(3), 335-347. <https://doi.org/10.12989/sss.2010.6.3.335>
- Devriendt, C. and Guillaume, P. (2008), "Identification of modal parameters from transmissibility measurements", *J. Sound Vib.*, **314**(1-2), 343-356. <https://doi.org/10.1016/j.jsv.2007.12.022>
- Dooms, D., Jansen, M., De Roeck, G., Degrande, G., Lombaert, G., Schevenels, M. and François, S. (2010), "StABIL: A Finite Element Toolbox for Matlab", *VERSION 2.0 USER'S GUIDE*.
- Farrar, C.R. and Worden, K. (2006), "An introduction to structural health monitoring", *Philosophical Transactions of the Royal Society A: Mathematical, Physical and Engineering Sciences*, **365**, 303-315.
- Fawcett, T. (2004), "ROC graphs: Notes and practical considerations for researchers", *Machine Learning*, **31**(1), 1-38.
- Guo, H., Zhuang, X. and Rabczuk, T. (2019), "A deep collocation method for the bending analysis of Kirchhoff plate", *CMC-COMPUTERS MATERIALS & CONTINUA*, **59**(2), 433-456.
- Hakim, S. and Razak, H.A. (2014), "Modal parameters based structural damage detection using artificial neural networks-a review", *Smart Struct. Syst., Int. J.*, **14**, 159-189. <https://doi.org/10.12989/sss.2014.14.2.159>
- Johnson, T.J. and Adams, D.E. (2002), "Transmissibility as a differential indicator of structural damage", *J. Vib. Acoust.*, **124**(4), 634-641. <https://doi.org/10.1115/1.1500744>
- Kaveh, A. and Maniati, M. (2015), "Damage detection based on MCSS and PSO using modal data", *Smart Struct. Syst., Int. J.*, **15**(5), 1253-1270. <https://doi.org/10.12989/sss.2015.15.5.1253>
- Koo, K.-Y., Brownjohn, J., List, D. and Cole, R. (2013), "Structural health monitoring of the Tamar suspension bridge", *Struct. Control Health Monitor.*, **20**(4), 609-625. <https://doi.org/10.1002/stc.1481>
- Lee, J.J., Lee, J.W., Yi, J.H., Yun, C.B. and Jung, H.Y. (2005), "Neural networks-based damage detection for bridges considering errors in baseline finite element models", *J. Sound Vib.*, **280**(3-5), 555-578. <https://doi.org/10.1016/j.jsv.2004.01.003>
- Maeck, J., Peeters, B. and De Roeck, G. (2001), "Damage identification on the Z24 bridge using vibration monitoring", *Smart Mater. Struct.*, **10**(3), 512. <https://doi.org/10.1088/0964-1726/10/3/314>
- Maia, N., Silva, J., Almas, E. and Sampaio, R. (2003), "Damage detection in structures: from mode shape to frequency response function methods", *Mech. Syst. Signal Process.*, **17**(3), 489-498. <https://doi.org/10.1006/mssp.2002.1506>
- Maia, N.M., Almeida, R.A., Urgueira, A.P. and Sampaio, R.P. (2011), "Damage detection and quantification using transmissibility", *Mech. Syst. Signal Process.*, **25**(7), 2475-2483. <https://doi.org/10.1016/j.ymsp.2011.04.002>
- Mehrhoj, M., Khaji, N., Moharrami, H. and Bahreininejad, A. (2008), "Damage detection of truss bridge joints using Artificial Neural Networks", *Expert Syst. Applicat.*, **35**(3), 1122-1131. <https://doi.org/10.1016/j.eswa.2007.08.008>
- Meruane, V. (2015), "Online sequential extreme learning machine for vibration-based damage assessment using transmissibility data", *J. Comput. Civil Eng.*, **30**(3), 04015042. [https://doi.org/10.1061/\(ASCE\)CP.1943-5487.0000517](https://doi.org/10.1061/(ASCE)CP.1943-5487.0000517)
- Nguyen, H.D., Bui, T.T., De Roeck, G. and Wahab, M.A. (2018), "Damage Detection in Simply Supported Beam Using Transmissibility and Auto-Associative Neural Network", *International Conference on Numerical Modelling in Engineering*, pp. 177-186.
- Nguyen, D.H., Bui, T.T., De Roeck, G. and Wahab, M.A. (2019a), "Damage detection in Ca-Non Bridge using transmissibility and artificial neural networks", *Struct. Eng. Mech., Int. J.*, **71**(2), 175-183. <https://doi.org/10.12989/sem.2019.71.2.175>
- Nguyen, T.Q., Nguyen, T.T., Nguyen-Xuan, H. and Ngo, N.K. (2019b), "A Correlation Coefficient Approach for Evaluation of Stiffness Degradation of Beams Under Moving Load", *Comput. Mater. Continua*, **61**(1), 27-53.
- Nguyen, T.Q., Tran, L.Q., Nguyen-Xuan, H. and Ngo, N.K. (2019c), "A statistical approach for evaluating crack defects in structures under dynamic responses", *Nondestruct. Test. Eval.*, 1-32. <https://doi.org/10.1080/10589759.2019.1699086>
- Peeters, B. and De Roeck, G. (2001), "One-year monitoring of the Z24-Bridge: environmental effects versus damage events", *Earthq. Eng. Struct. Dyn.*, **30**(2), 149-171. [https://doi.org/10.1002/1096-9845\(200102\)30:2<149::AID-EQE1>3.0.CO;2-Z](https://doi.org/10.1002/1096-9845(200102)30:2<149::AID-EQE1>3.0.CO;2-Z)
- Peeters, B., Maeck, J. and De Roeck, G. (2001), "Vibration-based damage detection in civil engineering: excitation sources and temperature effects", *Smart Mater. Struct.*, **10**(3), 518. <https://doi.org/10.1088/0964-1726/10/3/314>
- Roeck, G.D. (2003), "The state-of-the-art of damage detection by vibration monitoring: the SIMCES experience", *J. Struct. Control*, **10**(2), 127-134. <https://doi.org/10.1002/stc.20>
- Sahin, M. and Sheno, R. (2003), "Quantification and localisation of damage in beam-like structures by using artificial neural networks with experimental validation", *Eng. Struct.*, **25**(14), 1785-1802. <https://doi.org/10.1016/j.engstruct.2003.08.001>
- Sampaio, R., Maia, N., Ribeiro, A. and Silva, J. (2001), "Transmissibility techniques for damage detection", *Proceedings of the International Modal Analysis Conference*, pp. 1524-1527.
- Sanayei, M., Phelps, J.E., Sipple, J.D., Bell, E.S. and Brenner, B.R. (2011), "Instrumentation, nondestructive testing, and finite-element model updating for bridge evaluation using strain measurements", *J. Bridge Eng.*, **17**(1), 130-138. [https://doi.org/10.1061/\(ASCE\)BE.1943-5592.0000228](https://doi.org/10.1061/(ASCE)BE.1943-5592.0000228)
- Specht, D.F. (1991), "A general regression neural network", *IEEE Transact. Neural Networks*, **2**(6), 568-576.
- Thyagarajan, S., Schulz, M., Pai, P. and Chung, J. (1998), "Detecting structural damage using frequency response functions", *J. Sound Vib.*, **210**(1), 162-170.
- Tran-Ngoc, H., Khatir, S., De Roeck, G., Bui-Tien, T., Nguyen-Ngoc, L. and Abdel Wahab, M. (2018), "Model updating for Nam O bridge using particle swarm optimization algorithm and genetic algorithm", *Sensors*, **18**(12), 4131.

- <https://doi.org/10.2749/101686697780494563>
- Wahab, M.A. and De Roeck, G. (1997), "Effect of temperature on dynamic system parameters of a highway bridge", *Struct. Eng. Int.*, **7**(4), 266-270. <https://doi.org/10.2749/101686697780494563>
- Wahab, M.A. and De Roeck, G. (1999), "Damage detection in bridges using modal curvatures: application to a real damage scenario", *J. Sound Vib.*, **226**(2), 217-235. <https://doi.org/10.1006/jsvi.1999.2295>
- Weinstein, J.C., Sanayei, M. and Brenner, B.R. (2018), "Bridge damage identification using artificial neural networks", *J. Bridge Eng.*, **23**(11), 04018084. [https://doi.org/10.1061/\(ASCE\)BE.1943-5592.0001302](https://doi.org/10.1061/(ASCE)BE.1943-5592.0001302)
- Worden, K., Manson, G. and Allman, D. (2003), "Experimental validation of a structural health monitoring methodology: Part I. Novelty detection on a laboratory structure", *J. Sound Vib.*, **259**(2), 323-343. <https://doi.org/10.1006/jsvi.2002.5168>
- Wu, X., Ghaboussi, J. and Garrett Jr, J. (1992), "Use of neural networks in detection of structural damage", *Comput. Struct.*, **424**, 649-659. [https://doi.org/10.1016/0045-7949\(92\)90132-J](https://doi.org/10.1016/0045-7949(92)90132-J)
- Yan, Y., Cheng, L., Wu, Z. and Yam, L. (2007), "Development in vibration-based structural damage detection technique", *Mech. Syst. Signal Process.*, **21**(5), 2198-2211. <https://doi.org/10.1016/j.ymsp.2006.10.002>
- Yan, W.-J., Zhao, M.-Y., Sun, Q. and Ren, W.-X. (2019), "Transmissibility-based system identification for structural health Monitoring: Fundamentals, approaches, and applications", *Mech. Syst. Signal Process.*, **117**, 453-482. <https://doi.org/10.1016/j.ymsp.2018.06.053>
- Yeung, W. and Smith, J. (2005), "Damage detection in bridges using neural networks for pattern recognition of vibration signatures", *Eng. Struct.*, **27**(5), 685-698. <https://doi.org/10.1016/j.engstruct.2004.12.006>
- Zang, C. and Imregun, M. (2001), "Structural damage detection using artificial neural networks and measured FRF data reduced via principal component projection", *J. Sound Vib.*, **242**(5), 813-827. <https://doi.org/10.1006/jsvi.2000.3390>
- Zhou, Y.L. (2015), "Structural health monitoring by using transmissibility", *Industriales*.
- Zhou, Y.-L. and Abdel Wahab, M. (2017), "Damage detection using vibration data and dynamic transmissibility ensemble with auto-associative neural network", *Mechanika*, **23**, 688-695. <https://doi.org/10.5755/j01.mech.23.5.15339>
- Zhou, Y.-L. and Wahab, M.A. (2016), "Rapid early damage detection using transmissibility with distance measure analysis under unknown excitation in long-term health monitoring", *J. Vibroeng.*, **18**(7), 4491-4499. <https://doi.org/10.21595/jve.2016.17226>
- Zhou, Y.-L., Figueiredo, E., Maia, N. and Perera, R. (2015), "Damage detection and quantification using transmissibility coherence analysis", *Shock Vib.*, **2015**. <https://doi.org/10.1155/2015/290714>
- Zhou, Y.-L., Maia, N.M., Sampaio, R.P. and Wahab, M.A. (2017), "Structural damage detection using transmissibility together with hierarchical clustering analysis and similarity measure", *Struct. Health Monitor.*, **16**(6), 711-731. <https://doi.org/10.1177/1475921716680849>
- Zhou, Y.-L., Maia, N.M. and Abdel Wahab, M. (2018), "Damage detection using transmissibility compressed by principal component analysis enhanced with distance measure", *J. Vib. Control*, **24**(10), 2001-2019. <https://doi.org/10.1177/1077546316674544>